DYNAMIC JOINT PHY-MAC WAVEFORM DESIGN FOR IOT CONNECTIVITY

Konstantinos Tountas, George Sklivanitis, and Dimitris A. Pados

I-SENSE and Dept. of Computer and Electrical Eng. & Computer Science,
Florida Atlantic University, Boca Raton, FL, 33431
E-mail: {ktountas2017, gsklivanitis, dpados}@fau.edu

ABSTRACT

We envision dense network deployments of Internet-of-Things (IoT) connected devices that report data to a common base station (BS). The devices utilize repeats of a basic shaping pulse occupying the entire continuum of the device-accessible spectrum. We propose an optimal algorithm to adaptively design sparse waveforms with well-placed energy that maximize the signal-to-interference-plus-noise ratio (SINR) at the output of the maximum-SINR linear filter at the BS. Additionally, we propose a computationally efficient suboptimal waveform design algorithm for the same problem. Simulation studies show that the proposed waveform designs attain superior pre-detection SINR performance than conventional binary, quaternary, and sparse-binary/quaternary waveform designs, thus offering a promising PHY-MAC approach to maintain wireless connectivity in overloaded network setups.

Index Terms— Waveform design, channelization, all-spectrum, IoT, interference-avoidance

1. INTRODUCTION

Internet-of-Things (IoT) platforms will connect a huge number of machines and humans that produce, gather, share, and forward data. Drastically increasing data traffic from wirelessly connected "things" will significantly impact the design and implementation of next-generation wireless communication systems. Particularly, efficient spectrum and energy utilization in dense IoT network deployments entail joint optimization of communication parameters at the physical and medium-access-control (MAC) layers.

Interference avoidance via waveform design has attracted considerable attention toward the development of spectrally and energy efficient cognitive networks [1–4]. Particularly, a finite sequence of repeated square-root-raised cosine (SRRC) pulses that span the entire continuum of the device-accessible spectrum is optimized [1–4] to maximize the signal-to-interference-plus-noise ratio (SINR) at the output of the maximum-SINR receiver. Recent work in [5] considers binary antipodal and quaternary alphabets for the repeating sequence of pulses and evaluates the pre-detection SINR performance of max-SINR optimized digital waveforms in the presence of multiple access interference.

Recently proposed MAC protocol designs for IoT connectivity consider contention-based channel access. Work in [6] proposes a hybrid MAC scheme, where time-division multiple-access (TDMA) is proposed for voice packet transmissions that guarantee a packet loss-rate bound, while truncated CSMA/CA (T-CSMA/CA) is used by the devices to access the wireless channel. In [7] a hybrid slotted-CSMA/CA-TDMA protocol is proposed for dividing a logical frame into a contention-based slotted-CSMA/CA period and a contention-free slotted-TDMA period. On the other hand, joint PHY-MAC layer approaches for overloaded code-division multiple-access (CDMA) systems consider the design of non-orthogonal code waveforms to enable low complexity detection of multiple users communicating simultaneously over a common wireless channel. Recent work in [8] proposes both optimal and suboptimal computationally efficient algorithms for the adaptive design of sparse binary code waveforms. A statistical-mechanics framework for sparse CDMA in [9] demonstrates that small sparsity values offer considerable spectral-efficiency performance improvements.

In this paper, we envision dense network deployments of IoT connected devices that report data to a common base station (BS). We propose a joint PHY-MAC approach that leverages the design of interference avoiding waveforms. More specifically, IoT devices dynamically optimize a repeating sequence of basic shaping pulses that maximize the SINR at the output of the max-SINR receiver, and for the first time we consider adaptive sparse waveform designs with well-placed energy. In other words, the alphabet of the symbols of the proposed waveform designs does not have uniform energy distribution, and is optimized as the waveforms are designed. As a result, some symbols may have greater energy than others to account for multipath and/or intersymbol interference effects. The BS is responsible for dynamically sensing the spectrum environment, and updating the waveform designs of existing or new devices, to ensure network connectivity.

The rest of the paper is organized as follows. Section 2 presents the system model. Section 3 describes the waveform design problem. Section 4 evaluates the performance of the proposed waveform design in terms of pre-detection SINR, while a few concluding remarks are drawn in Section 5.

2. SYSTEM MODEL

We consider K single-antenna IoT devices transmitting information symbols to a single-antenna BS over a single-input single-output (SISO) flat fading channel with N resolvable paths. Each symbol $b_k[m], m = 1, 2, \dots, k = 1, 2, \dots, K$ is drawn from a unit energy, complex constellation $\mathcal{A}$, and is modulated by an all-spectrum digital waveform $s_k(t)$ of duration T. The transmitted signal of the k-th device is written as

$$x_k(t) \triangleq \sum_{m=0}^{\infty} \sqrt{P_k} b_k[m] s_k(t - mT) e^{j(2\pi f_c t + \phi_k)} \quad (1)$$

where $P_k > 0$ denotes the transmitted energy per symbol, ϕ_k is the carrier phase, and f_c is the carrier frequency of the m-th symbol for the k-th IoT device. The all-spectrum digital waveform $s_k(t)$ comprises L repeats of a basic shaping pulse (e.g. SRRC), each occupying the entire continuum of the device-accessible bandwidth, and is given by

$$s_k(t) \triangleq \sum_{l=0}^{L-1} \mathbf{d}_k[l] g_{T_c}(t - lT_c) \quad (2)$$

where $g_{T_c}(\cdot)$ is a SRRC shaping pulse of duration T_c, so that $T = LT_c$, and $\mathbf{d}_k$ is a unit-norm real/complex-valued [10] or binary/quaternary [1–5] code sequence of length L.

The transmitted signals propagate over Rayleigh fading multipath channels with N resolvable paths and experience additive Gaussian noise at the receiver. Multipath fading is modeled by a liner tapped-delay line with taps that are spaced at T_c intervals and are weighted by independent fading coefficients (i.e. Rayleigh distributed amplitude and uniformly distributed phase).

Without loss of generality, the carrier down-converted, pulse-matched filtered, and sampled received signal vector with respect to the k-th IoT user of interest in the presence of $K-1$ asynchronous single antenna users is written as

$$\mathbf{r}[m] \triangleq \sqrt{P_k} \mathbf{H}_k \mathbf{s}_k \, b_k[m] + \mathbf{y}_k \in \mathbb{C}^{L_N}, \quad m = 1, 2, \dots \quad (3)$$

where $L_N = L + N - 1$ is the multipath-extended symbol duration $L_N T_c$, and $\mathbf{H}_k \in \mathbb{C}^{L_N \times L}$ denotes the multipath channel matrix for the k-th IoT device defined as

$$\mathbf{H}_k \triangleq \begin{bmatrix} h_{k,1} & 0 & \cdots & 0 \\ h_{k,2} & h_{k,1} & \cdots & 0 \\ \vdots & \vdots & \cdots & \vdots \\ h_{k,N} & h_{k,N-1} & \cdots & 0 \\ 0 & h_{k,N} & \cdots & h_{k,1} \\ \vdots & \vdots & \cdots & \vdots \\ 0 & 0 & \cdots & h_{k,N} \end{bmatrix} \quad (4)$$

where $h_{k,n}, n = 1, 2, \dots, N$, is considered an independent zero-mean complex Gaussian random variable that models the n-th complex baseband channel coefficient for the k-th IoT device. With respect to the k-th IoT device, the total disturbance at the BS introduced by the rest of the $K-1$ devices is defined as

$$\mathbf{y}_k = \sum_{\substack{i=1 \\ i \neq k}}^{K} \sqrt{P_i} \mathbf{H}_i \mathbf{s}_i \, b_i[m] + \mathbf{n} \in \mathbb{C}^{L_N}, \quad m = 1, 2, \dots \quad (5)$$

where $\mathbf{n} \in \mathbb{C}^{L_N}$ models zero-mean additive white Gaussian noise with autocorrelation matrix $\mathbf{R}_n \triangleq \mathbb{E}\left\{\mathbf{n}\mathbf{n}^H\right\} = \sigma^2 \mathbf{I}_{L_N}$ and the autocorrelation matrix of the total disturbance is defined as $\mathbf{R}_k \triangleq \mathbb{E}\left\{\mathbf{y}_k \mathbf{y}_k^H\right\} \in \mathbb{C}^{L_N \times L_N}$.

Assuming perfect knowledge of the total disturbance autocorrelation matrix at the BS, the linear filter $\mathbf{w}_k \in \mathbb{C}^{L \times 1}$ that exhibits maximum output SINR at the receiver can be found to be any scaled version of $\mathbf{w}_{\max-\mathrm{SINR}}(\mathbf{s}_k) = c\mathbf{R}_k^{-1}\mathbf{H}_k\mathbf{s}_k$, $c > 0$ for any waveform $\mathbf{s}_k$ with $\|\mathbf{s}_k\| = 1$. The post-filtering SINR at the output of the maximum-SINR receiver filter is then written as

$$\begin{aligned} \mathrm{SINR}(\mathbf{s}_k) &\triangleq \frac{\mathbb{E}\left\{\left|\mathbf{w}_{\max-\mathrm{SINR}}^H(\mathbf{s}_k)\left(\sqrt{P_k}\mathbf{H}_k\mathbf{s}_k b_k[m]\right)\right|^2\right\}}{\mathbb{E}\left\{\left|\mathbf{w}_{\max-\mathrm{SINR}}^H(\mathbf{s}_k)\,\mathbf{y}_k\right|^2\right\}} \\ &= P_k \mathbf{s}_k^H \mathbf{H}_k^H \mathbf{R}_k^{-1} \mathbf{H}_k \mathbf{s}_k. \end{aligned} \quad (6)$$

Our goal at the BS is to find a waveform $\mathbf{s}_k$ that maximizes pre-detection $\mathrm{SINR}(\mathbf{s}_k)$ for the k-th user of interest. We define $\mathbf{W}_k \triangleq \mathbf{H}_k^H \mathbf{R}_k^{-1} \mathbf{H}_k$. Assuming that $\mathbf{s}_k \in \mathbb{C}^L$, since $\mathbf{W}_k \succ 0$, the complex-valued waveform that maximizes the post-filtering SINR is given by

$$\mathbf{s}_{k,\mathbb{C}-\mathrm{OPT}} = \underset{\mathbf{s} \in \mathbb{C}^L, \|\mathbf{s}\|=1}{\operatorname{argmax}} \; P_k \mathbf{s}^H \mathbf{W}_k \mathbf{s} = \mathbf{q}_1 \quad (7)$$

where $\mathbf{q}_1, \mathbf{q}_2, \dots, \mathbf{q}_L$ denote the eigenvectors of $\mathbf{W}_k$ with corresponding eigenvalues $\lambda_1 \geq \lambda_2 \geq \cdots \geq \lambda_L > 0$. In this work, our objective is to find a waveform $\mathbf{s}_k$ takes values from a finite-element complex alphabet with well-placed energy per element to maximize pre-detection SINR.

3. PROPOSED SPARSE VARIABLE ALPHABET WAVEFORM DESIGN

3.1. Problem Formulation

We begin the problem formulation by noting that due to chip-level disturbance correlations, there may exist chip transmission intervals wherein the k-th device should avoid to transmit or utilize less energy. As a result, transmission energy should be adaptively distributed to each transmission interval to maintain wireless connectivity. In this work, the waveform $\mathbf{s}_k$ of the k-th IoT device can take values from the finite alphabet $\{0, \pm\{\alpha, \beta\} \pm \{\alpha, \beta\} j\}$, where $\alpha, \beta \in \mathbb{R}^+$, where parameters α and β control the inter-chip energy. The constellation of the proposed waveform is depicted in Fig. 1. The

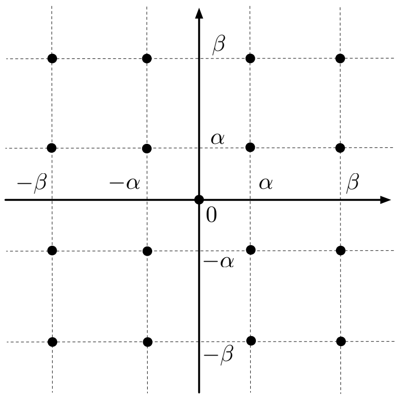

Fig. 1. Proposed waveform constellation.

max-SINR waveform design problem is therefore written as

$$\tilde{\mathbf{s}}_k \triangleq \underset{\substack{\mathbf{s}\in\{0,\pm\{\alpha,\beta\}\pm\{\alpha,\beta\}j\}^L \\ \|\mathbf{s}\|=1}}{\operatorname{argmax}} P_k\, \mathbf{s}^H \mathbf{W}_k \mathbf{s}. \tag{8}$$

In the rest of our algorithmic developments we assume sparsity up to $L/2$, i.e. the IoT device may not transmit/remain silent up to half of the total available chip transmission intervals and utilize the rest of intervals for transmission.

3.2. Optimal Algorithm

The waveform design problem in (8) is a combinatorial optimization problem and its optimal solution can be acquired by exhaustively searching over the waveform feasibility set. More specifically, we first rewrite the optimization problem in (8) as

$$\max_{c\in\{\alpha,\beta\}} \max_{\substack{\mathbf{s}\in\{0,\pm c\pm cj\}^L \\ c^2\|\mathbf{s}\|_0=1}} \mathbf{s}^H \mathbf{W}_k \mathbf{s} \tag{9}$$

$$= \max_{c\in\{\alpha,\beta\}} \max_{V\in[L]} \max_{\substack{\mathbf{s}\in\{0,\pm c\pm cj\}^L, \\ \|\mathbf{s}\|_0=V, \|\mathbf{s}\|=1}} \mathbf{s}^H \mathbf{W}_k \mathbf{s} \tag{10}$$

where $[L] \triangleq \{L/2, \ldots, L\}$ is the allowed waveform sparsity, and $\|\cdot\|_0$ returns the number of the non-zero elements of the input vector. The solution to (10) can be found by two nested exhaustive searches. For every $V \in [L]$, we solve the inner maximization problem in (10) to obtain

$$\tilde{\mathbf{s}}_{k,V} \triangleq \underset{\substack{\mathbf{s}\in\{0,\pm c\pm cj\}^L, \\ \|\mathbf{s}\|_0=V, \|\mathbf{s}\|=1}}{\operatorname{argmax}} \mathbf{s}^H \mathbf{W}_k \mathbf{s}. \tag{11}$$

We search exhaustively for all $\binom{L}{V}4^V$ sequences in the feasibility set of (11). For each sequence, we create all the possible combinations for $c \in \{\alpha, \beta\}$, which results to a total of $\binom{L}{V}16^V$ sequences. Given that $\|\tilde{\mathbf{s}}_{k,V}\| = 1$ we then search for $\alpha, \beta \in \mathbb{R}^+$ parameters that maximize pre-detection SINR.

Algorithm 1 Suboptimal Iterative Algorithm

Input: $\mathbf{W}_k = P_k\, \mathbf{H}_k^H \mathbf{R}_k^{-1} \mathbf{H}_k$, $c \in \mathbb{R}^+$

$\quad \mathbf{Q}_k \leftarrow \mathrm{EVD}(\mathbf{W}_k)$

$\quad$ **for** $V \in \{L/2, \ldots, L\}$ **do**

$\quad\quad \mathbf{a} \leftarrow$ arbitrary in $\mathbb{C}^L$, with $\|\mathbf{a}\| = 1$; $m \leftarrow 0$

$\quad\quad$ **while** not converged **do**

$\quad\quad\quad \mathbf{s} \leftarrow c\left\{\mathrm{sgn}\left[I_V\left(\mathrm{Re}\left\{\mathbf{W}_k^H \mathbf{a}\right\}\right)\right] + j\mathrm{sgn}\left[I_V\left(\mathrm{Im}\left\{\mathbf{Q}_k^H \mathbf{a}\right\}\right)\right]\right\}$

$\quad\quad\quad \mathbf{a} \leftarrow \frac{\mathbf{Q}_k \mathbf{s}}{\|\mathbf{Q}_k \mathbf{s}\|}$

$\quad\quad\quad m' \leftarrow \mathbf{s}_k^H \mathbf{W}_k \mathbf{s}$

$\quad\quad\quad$ **if** $m' - m \leq \mathrm{threshold}$ **then**

$\quad\quad\quad\quad \mathbf{s}_{k,V} \leftarrow \mathbf{s}$

$\quad\quad\quad\quad m \leftarrow m'$

$\quad\quad\quad$ **end if**

$\quad\quad$ **end while**

$\quad$ **end for**

$\quad \tilde{\mathbf{s}}_{k,V}^{\mathrm{IT}} \leftarrow \max_{\mathbf{s}\in\left\{\mathbf{s}_{k,L/2},\ldots,\mathbf{s}_{k,L}\right\}} \mathbf{s}^H \mathbf{W}_k \mathbf{s}$

Finally, we obtain $\tilde{\mathbf{s}}_k^{\mathrm{Exh}}$ by solving

$$\tilde{\mathbf{s}}_k^{\mathrm{Exh}} = \underset{\mathbf{s}\in\left\{\tilde{\mathbf{s}}_{k,1},\tilde{\mathbf{s}}_{k,2},\ldots,\tilde{\mathbf{s}}_{k,L/2}\right\}}{\operatorname{argmax}} P_k\, \mathbf{s}^H \mathbf{H}_k^H \mathbf{R}_k^{-1} \mathbf{H}_k \mathbf{s}. \tag{12}$$

3.3. Suboptimal Algorithm

The complexity of the optimal algorithm presented above is prohibitive for practical applications where L is large. In this section, we propose to separate the waveform design and energy distribution problems, and present a suboptimal iterative algorithm for solving the waveform design problem in a computationally efficient way.

We focus on (11) and start by decomposing $\mathbf{W}_k$ by means of eigenvalue decomposition as $\mathbf{W}_k = \mathbf{Q}_k^H \mathbf{Q}_k$ for some $\mathbf{Q}_k \in \mathbb{C}^{L\times L}$. Then, by the Cauchy-Schwarz inequality [11]

$$\max_{\substack{\mathbf{s}\in\{0,\pm c\pm cj\}^L, \\ \|\mathbf{s}\|_0=V, \|\mathbf{s}\|=1}} \mathbf{s}^H \mathbf{W}_k \mathbf{s} = \max_{\substack{\mathbf{s}\in\{0,\pm c\pm cj\}^L, \\ \|\mathbf{s}\|_0=V, \|\mathbf{s}\|=1}} \max_{\substack{\mathbf{a}\in\mathbb{C}^L, \\ \|\mathbf{a}\|=1}} \mathbf{s}^H \mathbf{Q}_k \mathbf{a}. \tag{13}$$

For any given $\mathbf{s}$ in the feasibility set of the outer maximization in (13), the inner maximization is achieved for

$$\mathbf{a} = \frac{\mathbf{Q}_k \mathbf{s}}{\|\mathbf{Q}_k \mathbf{s}\|}. \tag{14}$$

For any given $\mathbf{a}$ in the feasibility set of the inner maximization in (13), the outer maximization is achieved for

$$\mathbf{s}_k = c\left\{\mathrm{sgn}\left[I_V\left(\mathrm{Re}\left\{\mathbf{Q}_k^H \mathbf{a}\right\}\right)\right] + j\mathrm{sgn}\left[I_V\left(\mathrm{Im}\left\{\mathbf{Q}_k^H \mathbf{a}\right\}\right)\right]\right\} \tag{15}$$

where $\mathrm{sgn}(\cdot)$ returns the sign of its arguments (note that $\mathrm{sgn}(0) = 0$), and $I_V(\cdot)$ returns its arguments after setting

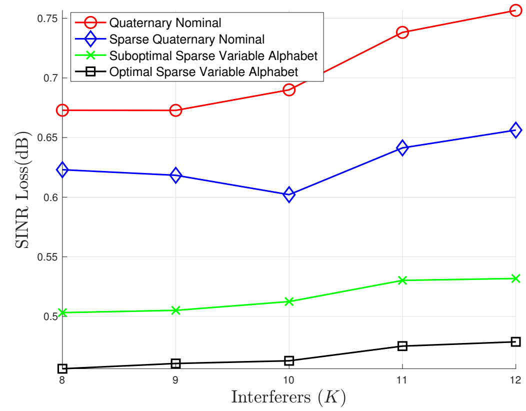

Fig. 2. SINR loss as a function of the number of users ($L = 6$, N = 4, $\mathrm{SNR}_1 = 10$ dB).

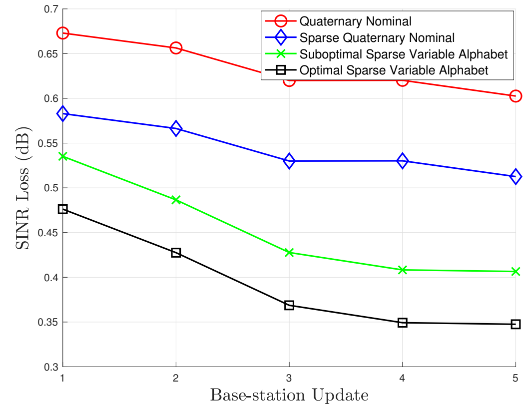

Fig. 3. SINR loss as a function of waveform updates ($L = 6$, $N = 4$, $K = 8$).

to zero the $L - V$ entries with the lowest absolute values. For every $V \in [L]$, the algorithm initializes at some arbitrary $\mathbf{a}_V^{(0)}, \left\|\mathbf{a}_V^{(0)}\right\| = 1$ and produces a sequence of points in the feasibility set of (11), $\left\{\mathbf{s}_V^{(t)}\right\}, t = 1, 2, \ldots$. At the t-th step, $t > 0$, the algorithm calculates

$$\mathbf{s}_V^{(t)} = c\left\{\mathrm{sgn}\left[I_V\left(\mathrm{Re}\left\{\mathbf{W}_k^H\mathbf{a}\right\}\right)\right] + j\mathrm{sgn}\left[I_V\left(\mathrm{Im}\left\{\mathbf{Q}_k^H\mathbf{a}\right\}\right)\right]\right\} \quad (16)$$

$$\mathbf{a}_V^{(t)} = \frac{\mathbf{Q}_k\mathbf{s}_V^{(t)}}{\left\|\mathbf{Q}_k\mathbf{s}_V^{(t)}\right\|}. \quad (17)$$

After obtaining a convergence point $\mathbf{s}_V$ the algorithm returns the approximate solution to (11) by solving

$$\tilde{\mathbf{s}}_{k,V}^{\mathrm{IT}} = \underset{\mathbf{s}\in\left\{\mathbf{s}_{k,L/2},\ldots,\mathbf{s}_{k,L}\right\}}{\mathrm{argmax}} \mathbf{s}^H\mathbf{W}_k\mathbf{s}. \quad (18)$$

Algorithm 1 offers a pseudocode for the proposed suboptimal iterative waveform design. After the iterative procedure produces the best approximation of the sparse waveform, we search exhaustively for the best combinations of values for parameters α and β.

4. SIMULATION STUDIES

We consider a star network topology with varying number of IoT devices that utilize waveforms of length $L = 6$ to report data to a BS. We assume that the transmitted signals propagate over multipath fading channels with $N = 4$ resolvable paths. The signal-to-noise ratio (SNR) of the device-of-interest is set to $\mathrm{SNR}_1 \triangleq \frac{P_1}{\sigma^2} = 10$ dB, while the SNR of the other devices $\mathrm{SNR}_k \triangleq \frac{P_k}{\sigma^2}, k = 2, \ldots, K$ is distributed uniformly between 8dB and 11dB. We evaluate the pre-detection SINR loss of (i) the proposed suboptimal sparse waveform design with variable amplitude; (ii) the optimal sparse waveform design with variable amplitude; (iii) the optimal sparse-quaternary waveform; and (iv) the optimal quaternary waveform with nominal alphabet (uniformly distributed energy), with respect to the optimal, complex waveform given by (7). In both (iii) and (iv) the waveforms are obtained by exhaustive search over all possible sequences.

In Fig. 2, we plot the SINR loss as a function of the number of devices K that varies from 8 to 12. We observe that the proposed optimal and suboptimal waveform designs offer superior pre-detection SINR performance compared to the nominal quaternary and sparse-quaternary waveform designs. Additionally, the proposed waveform designs achieve post-filtering SINR performance that is closer to the SINR performance of the complex eigenvector maximizer. Fig. 3 depicts the SINR loss as a function of the number of updates performed iteratively by the base-station optimizing sequentially the waveforms of $K = 8$ devices. The SNR of the IoT devices is uniformly distributed between 8 dB and 11 dB. We observe that the proposed waveform designs offer superior pre-detection SINR performance than the nominal quaternary and sparse-quaternary waveforms.

5. CONCLUSIONS

We present max-SINR sparse waveforms with carefully placed energy to efficiently utilize spectrum and energy resources in future IoT dense network deployments. We propose an optimal waveform design algorithm and a suboptimal computationally efficient algorithm for practical applications that require the implementation of waveforms with long code lengths. Simulation studies demonstrate that the proposed waveform designs outperform (in pre-detection SINR) conventional non-sparse and sparse waveform designs based on nominal alphabet designs. Finally, optimal sparse waveform designs with variable alphabets can achieve pre-detection SINR performance that is closer to the SINR performance of the max-SINR optimal complex-valued waveform.

6. REFERENCES

[1] G. Sklivanitis, A. Gannon, K. Tountas, D. A. Pados, S. N. Batalama, S. Reichhart, M. Medley, N. Thawdar, U. Lee, J. D. Matyjas, S. Pudlewski, A. Drozd, A. Amanna, F. Latus, Z. Goldsmith, and D. Diaz, "Airborne cognitive networking: Design, development, and deployment," *IEEE Access*, vol. 6, pp. 47 217–47 239, Jul. 2018.

[2] L. Ding, K. Gao, T. Melodia, S. N. Batalama, D. A. Pados, and J. D. Matyjas, "All-spectrum cognitive networking through joint distributed channelization and routing," *IEEE Trans. Wireless Commun.*, vol. 12, no. 11, pp. 5394–5405, Nov. 2013.

[3] K. Gao, S. N. Batalama, D. A. Pados, and J. D. Matyjas, "Cognitive code-division channelization," *IEEE Trans. Wireless Commun.*, vol. 10, no. 4, pp. 1090–1097, Apr. 2011.

[4] G. Sklivanitis, E. Demirors, A. M. Gannon, S. N. Batalama, D. A. Pados, and T. Melodia, "All-spectrum cognitive channelization around narrowband and wideband primary stations," in *Proc. IEEE Global Commun. Conf. (Globecom)*, San Diego, CA, Dec. 2015.

[5] K. Tountas, G. Sklivanitis, D. A. Pados, and S. N. Batalama, "All-spectrum digital waveform design via bit flipping," in *Proc. IEEE Global Commun. Conf. (Globecom)*, Abu Dhabi, UAE, Dec. 2018, to appear.

[6] Q. Ye and W. Zhuang, "Distributed and adaptive medium access control for internet-of-things-enabled mobile networks," *IEEE Internet of Things Journal*, vol. 4, no. 2, pp. 446–460, April 2017.

[7] N. Shahin, R. Ali, and Y. Kim, "Hybrid slotted-csma/ca-tdma for efficient massive registration of iot devices," *IEEE Access*, vol. 6, pp. 18 366–18 382, 2018.

[8] G. Sklivanitis, P. P. Markopoulos, S. N. Batalama, and D. A. Pados, "Sparse waveform design for all-spectrum channelization," in *2017 IEEE International Conference on Acoustics, Speech and Signal Processing (ICASSP)*, March 2017, pp. 3764–3768.

[9] M. Yoshida and T. Tanaka, "Analysis of sparsely-spread cdma via statistical mechanics," in *2006 IEEE International Symposium on Information Theory*, July 2006, pp. 2378–2382.

[10] S. Ulukus and R. D. Yates, "User capacity of asynchronous cdma systems with matched filter receivers and optimum signature sequences," *IEEE Transactions on Information Theory*, vol. 50, no. 5, pp. 903–909, May 2004.

[11] G. H. Golub and C. F. Van Loan, *Matrix Computations (3rd Ed.)*. Baltimore, MD: Johns Hopkins University Press, 1996.